

Emission of X-ray from 1kJ Plasma Focus Device and its Preliminary Applications

F. Diab and G. M. El-Kashef*

Plasma and Nuclear Fusion Department, Nuclear Research Center, Atomic Energy Authority, Egypt.

Received: 21 Feb. 2016, Revised: 22 Mar. 2016, Accepted: 24 Mar. 2016.

Published online: 1 Jul. 2016.

Abstract: A 1kJ Mother Type plasma focus (PF) device has been designed and constructed and energized by 30.84 μ f capacitors charged up to 8 kV giving a peak discharge current up to 150 kA, with rise time of 3 μ Sec. The PF in this work is reported as a pulsed and rich source of X-ray, operated with Argon at a filling pressure in the range of 0.2 to 2 torr. The measurement and analysis of X-ray emitted from 1 kJ PF device has been carried out using a PIN diode, light guide, aluminum filter with different thicknesses. The X-ray emission produced by the PF discharge is investigated. From the experimental results it is found that with increasing the pressure greater than 0.7 torr, very consistent and high output of X-ray radiation is recorded, at the peak of the discharge current and voltage. Multiple X-ray spikes corresponding to different voltage spikes at different instants have been observed. In order to determine the electron temperature of the plasma an indirect method was used by a PIN diode detector coupled with Al foil of different thicknesses. The result shows that the electron temperature of the plasma is ranged between 0.5 to 3 keV, when the operating pressure is 0.7 torr and charging voltage is 8 kV. Some physical properties of Polytetrafluoroethylene (PTFE) films were studied. Therefore, in the present work, the change in the surface free energy of (PTFE) samples is reported. X-Ray Florescence (XRF) analysis showed that, there are some new elements appeared on the surface of the sample after exposed to the ion beam, these elements and their concentrations are recorded.

Keywords: Plasma Focus devices, Mather type plasma focus, Argon gas pressure, X -ray emissions, voltage spike

1 Introduction

Plasma Focus (PF) device was developed in the earlier 60s [1] and it found to be a rich plasma source of multi radiation. PF discharge produces short-lived plasma that is of high temperature and high density by making use of the self-generated magnetic field through electromagnetic acceleration and compression [1]. In this work a Mather type PF device has been used, it has been widely studied because of its low cost, simplicity of engineering, various radiation and small dimensions in comparison with other radiation sources [2]. This device was primarily constructed to study the X-ray generation and possible enhancement. The sort of radiation depends on the type of gases inside the reactor, material of electrodes, geometry and other parameters [2]. The PF is a device consisting of coaxial electrodes inside a vessel containing a mixture of gases at a pressure less than several torr. The PF machines are pulsed electrical discharge in gases in which micron stabilities and turbulence lead to the generation of powerful beams of electrons, ions and emissions a large number of X-ray. The properties of the soft X-rays emission from the PF are reported, and in recent years there is considerable interest in developing the plasma focus into a high-brightness source. The detailed characteristics of the X-ray emission of a given

focus device depend in a rather complicated way on the design and operating parameters of the PF device (such as the storage energy, the plasma current, and the driver impedance; the electrode and insulator material, shape and configuration; gas pressure and composition [1]). Plasma focus machine are pulsed electrical discharges in gases in which micronic stabilities and turbulence lead to the generation of powerful beam of electrons and ions and the emission of a large numbers of X-rays [3].

In the last years the investigations related to the emissions of X-ray from PF devices have been reported to (a) characterization of both soft and hard X-rays from the plasma column and hot-spots in discharges operating with gases with atomic number higher than hydrogen (neon, argon, xenon, etc) and mixtures of gases that is in soft X-ray, in hard X-ray characterization of the interactions of energetic electron beams impacting on the anode; (b) the PF as an x-ray source for applications and (c) X-ray studies using composite loads in PF devices as gas puffed PF and wire in PF discharges [4]. This has led to an increasing interest in exploiting the PF device. The X-ray emissions from PF devices have been explored over the wide range of capacitor bank energies ranging from large megajoule and

*Corresponding author e-mail: fatheyd@yahoo.co.uk

few hundred kilojoule banks to medium sized kilojoule banks to subkilojoule banks of miniature sized focus devices [5].

2 Experimental Setup and Diagnostics

The schematic arrangements of a Mather type PF chamber and electrode system is shown in Figure 1. The experiment procedures were carried out on the Mather-type PF device, it designed and constructed at Plasma and Nuclear Fusion Department, Nuclear Research Center, Atomic Energy Authority, Egypt. This system is energized by a capacitor bank consists of four capacitor which are connected in parallel and has a capacitance of 30.84 μf and charged up to 8 kV giving a peak discharge current up to 150 kA. To initiate the discharge through the electrodes a high voltage trigger was located near the spark gap which is a vital element since it is responsible to start the breakdown just before the shots. The cleaning process of the spark gap is carried out before and after 5 shots.

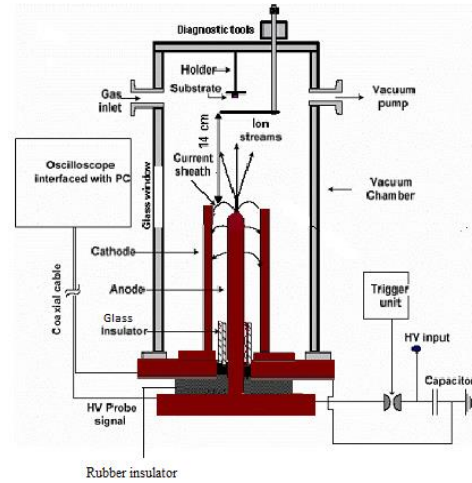
The discharge chamber is made of stainless steel and it has a length of 40 cm and diameter of 38 cm. The electrodes of the PF device in this experiment are a solid cylindrical tube to a void the excessive hard X-ray emission from the anode surface due to electron bombardment. The position of cathode electrodes around the anode was completely symmetrical and provided a cathode to anode radius ratio of 3.5.

In details, the electrodes system consists of a central solid copper anode of 130 mm length and 40 mm diameter, and a cathode consisting of eight copper rods each of 140 mm length and 10 mm diameter arranged in a circle of 140 mm diameter concentric with the anode as shown in figure 1(b). The length of the individual cathode rod is 140 mm with 10 mm higher than the length of anode rod. The anode is insulated from the cathode at the back wall by a Pyrex glass tube of 50 mm length, 2.5 mm thick and 44 mm diameter. This glass insulator plays an important role in the symmetrical formation of the current sheet and has to be properly mounted to avoid being broken by vibration. This glass insulator is mounted in a rubber holder which is acts as a vacuum and high voltage seal.

The PF is operated with argon as the working gas. The device was evacuated to lower than 0.3 torr before puffing argon gas by rotary van pump and filled with the required gas (argon) to a particular pressure (0.2–2 torr) before operation. This level of vacuum proved to be sufficient for operating with good focus in argon gas. In order to reduce and clean the vacuum chamber from impurities and contamination, the chamber is refreshed after every 8 shots and fresh argon gas is refilled to the desired pressure [6]

Figure1 (b) shows the electrode system of the device with removed discharge chamber. The current in the discharge circuit and the voltage across the PF tube versus time during the PF discharge are monitored by a Rogowski coil and an

ohmic voltage divider probe, respectively. The signals from the voltage divider and the current monitor were recorded in a digitizing oscilloscope (Tektronix 2014,100 MHz).



(a)



(b)

Fig.1 (a) the schematic diagram of the PF device and its electrical circuits (b) Mather's type electrode system; center anode, eight cathode rods and Pyrex insulator.

3 Results and Discussion

Experiments are carried out on the PF system to study the effect of operating pressure on the X-ray emission from argon plasma. The argon gas pressure is varied from 0.3 to 2 Torr, for each value of pressure 5 discharges is performed and the simultaneous current, voltage and X-ray signals are recorded for each shot. The optimized pressure for good focusing in present case is 0.7 torr in argon medium. At the optimum conditions, the signal shows a sharp increase in the output voltage at this time and pressure to confirm an intense compression at the time of focusing as shown in figure 3.

3.1 Measurements of Discharge Current and Voltage

The total discharge current and voltage was measured by a Rogowski coil and high voltage probe respectively. The typical signals of Rogowski coil and high voltage probe are shown in figure 3. According to figure 3, the maximum pinch compression should be nearly coincident approximately with the peak current in order to achieve the best efficiency.

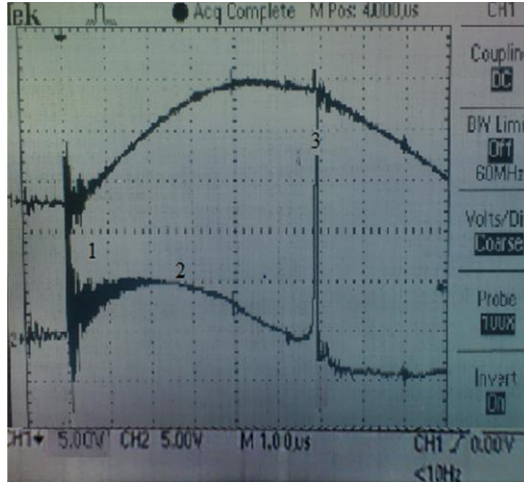


Fig.3: Typical waveforms of the current (upper trace) and voltage (lower trace) (time scale 1μS/div) signals showing the plasma focus effect

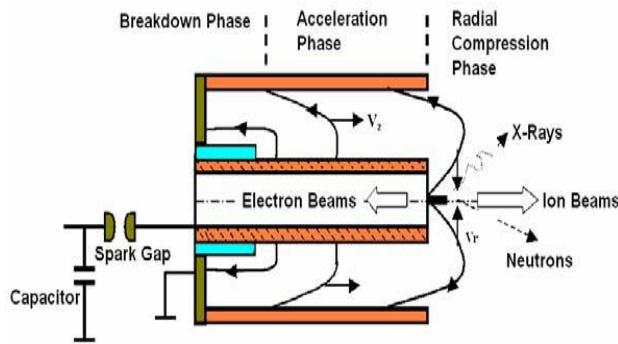


Fig.4 Mather type of the PF device showing the three phases of PF discharge.

Figure 3 shows the typical signals of discharge voltage and the discharge current at charging voltage 8 kV showing the optimum operating conditions for argon gas pressures. When plasma focus loaded, the current waveform distorts from damped sinusoid due to electrodynamic effects of plasma motion. The spikes of measured current waveform indicate that the pinch phase starts. The oscilloscopic traces of the voltage probe and current signals for a typical plasma focus shot 0.7 torr are shown in figure 3. The time history of all filling gas pressures shows that the first peak (labelled 1) of the voltage probe signal corresponds to the surface breakdown across insulator sleeve, and the relatively long flat part and the second peak afterwards (labelled 2) correspond to the axial acceleration phase and the third peak afterwards (labelled 3) correspond to the radial collapse

phase of the plasma focus. These three phases of PF discharge are described in figure 4.

Figure 4 shows a scheme of the PF circuit and the plasma dynamics. The capacitor C is discharged over the electrode through a spark gap. The plasma dynamics is sketched in a side section of the electrodes (Breakdown phase). The discharge starts over the insulator (Acceleration phase) the current sheath is accelerated along the coaxial electrodes, and IV: pinch (Radial compression phase).

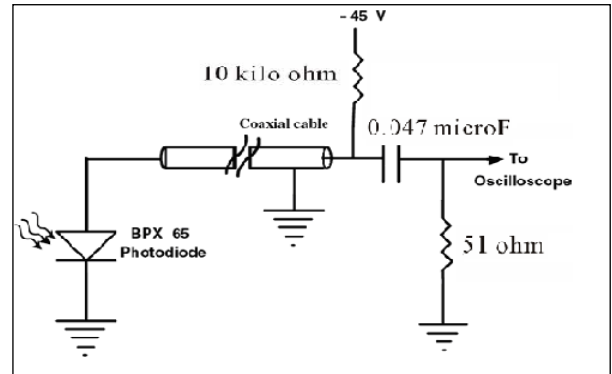


Fig. 5, the basic circuit of the BXP65 PIN photodiode

Figure 5 shows the bias circuit of the BXP65 diode which can be seen the PIN diodes are reverse biased at -45 volts. This circuit is a diagnostic for recording the X-ray emissions.

The optimum operating conditions in this PF device

As can be seen from figure 3 the discharge starts along the insulator sleeve surface (breaks down) and turn the filling gas to the electrically conducting gas which is called current sheath. Radial current sheath accelerates towards the open end of the anode and collects the gas in front of it by Lorentz force (axial acceleration phase). When the current sheath arrives at the anode end, it is rapidly compressed in the radial direction and finally focuses into a dens plasma column (pinch) at the top of the anode. In order to reduce the effect of plasma impurities contamination, the chamber was pumped out and filled with fresh gas every 8 shots.

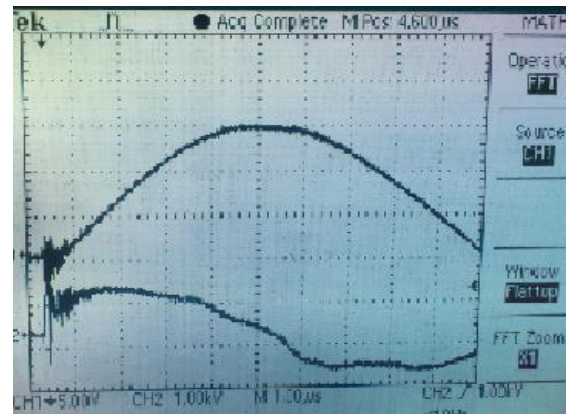


Fig.6(a)- $V_{ch} = 8kV$ and $P=2$ torr

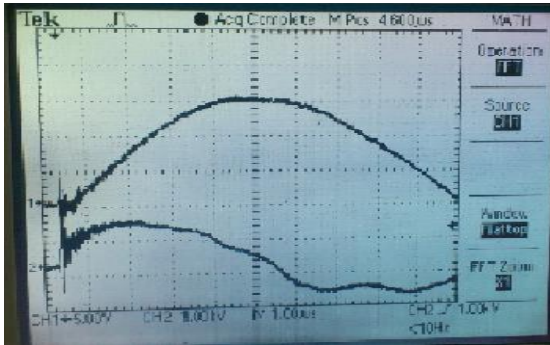


Fig.6(b)- $V_{ch} = 8\text{ kV}$ and $P=1.5\text{ torr}$

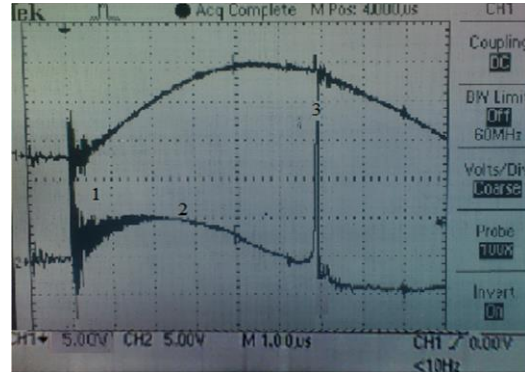


Fig.6(f)- $V_{ch} = 8\text{ kV}$ and $P=0.7\text{ torr}$

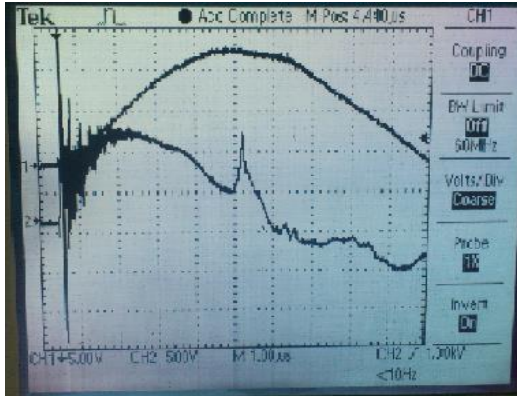


Fig.6(c)- $V_{ch} = 8\text{ kV}$ and $P=1\text{ torr}$

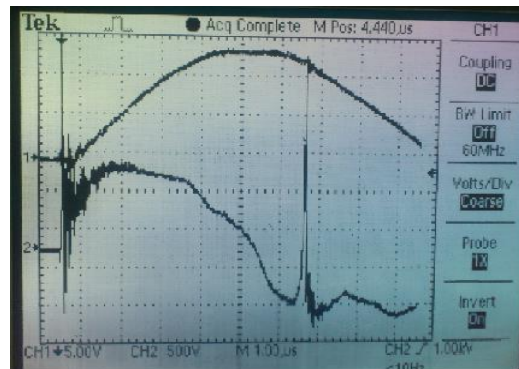


Fig.6(g)- $V_{ch} = 8\text{ kV}$ and $P=0.6\text{ torr}$

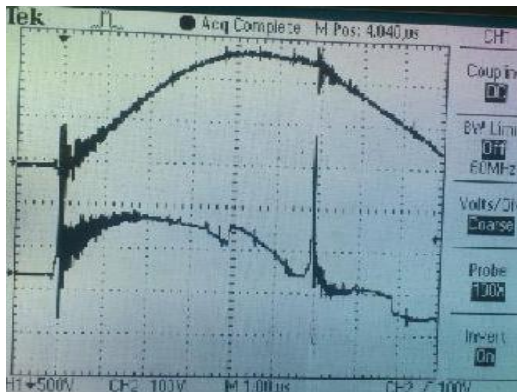


Fig.6(d)- $V_{ch} = 8\text{ kV}$ and $P=0.9\text{ torr}$

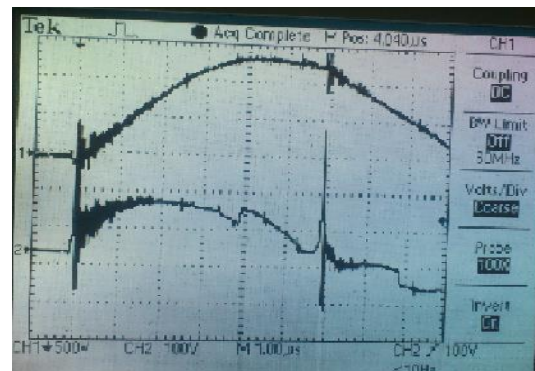


Fig.6(h)- $V_{ch} = 8\text{ kV}$ and $P=0.5\text{ torr}$

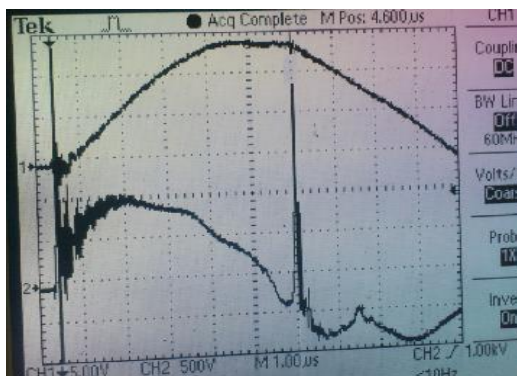


Fig.6(e)- $V_{ch} = 8\text{ kV}$ and $P=0.8\text{ torr}$

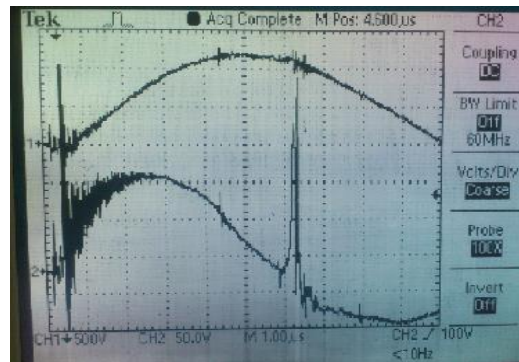


Fig.6(i)- $V_{ch} = 8\text{ kV}$ and $P=0.4\text{ torr}$

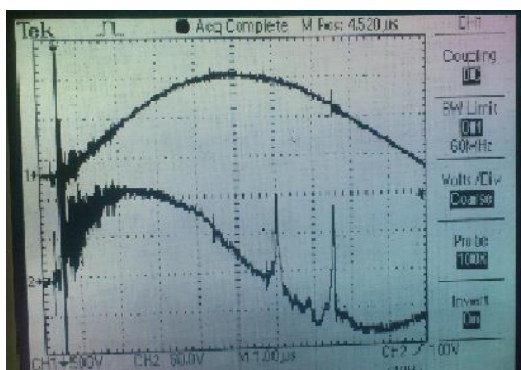


Fig.6(j)- $V_{ch} = 8\text{ kV}$ and $P=0.3$ torr

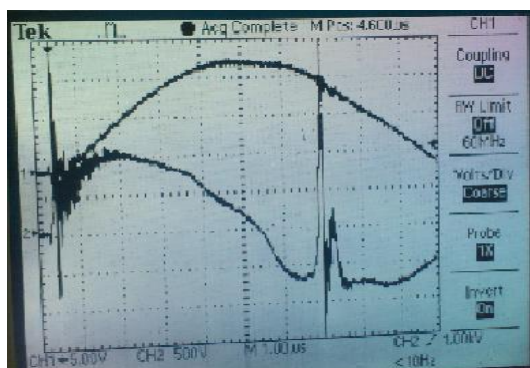


Fig.6(k)- $V_{ch} = 8\text{ kV}$ and $P=0.2$ torr

Fig. 6(a,b,c,d,e,f,g,h,i,j and k) shows the typical PF current waveform (upper trace) and the voltage (lower trace) measured by Rogowski coil and high voltage probe respectively, with the time scale of ($1\mu\text{S}/\text{div}$).

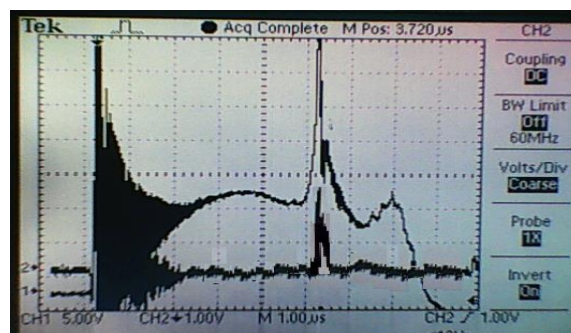
For this experiment low pressures from 0.2 to 1 Torr were generally found to be sufficient in order to generate a plasma focus with different intensity. Due to the optimization of the focus as shown in the above figures, the sinusoidal current and the discharge voltage characteristics for the short-circuit discharges were measured using a high voltage probe and Rogowski coil respectively. In principle, any focus system shows this kind of sinusoidal behavior due to its short-cut nature. It corresponds to the case that the plasma current inside the chamber oscillates between two electrodes. In this frame, once a critical damping case is caught, the oscillations decay and a smooth discharge regime appears as usual. The decrease in the current curve proved the inductance increase by the formation of plasma between the electrodes.

Figure 6 from (a to k) shows typical PF current and voltage. The discharge voltage is fixed at 8 kv. As can be seen from this figure no focusing appear at figure 6(a and b), while starting from figure 6(c) a weak focusing is obtained at 1 torr. At 0.9 torr and 0.8 torr a spike in the voltage discharge is appearing and good breakdown is obtained. Very good focusing is obtained at 0.7 torr. As can be seen from these figures the spikes starting with the pressure increase, the spikes in the voltage become more intense as the pressure is

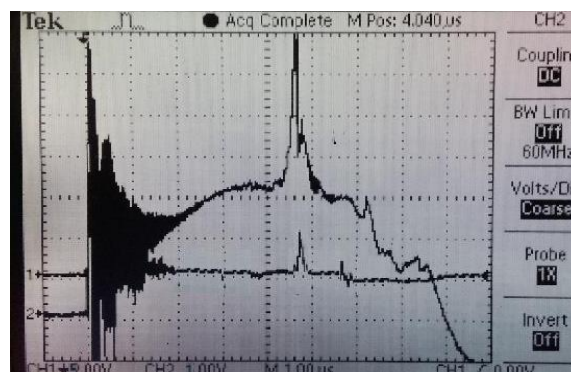
more increased. At still higher pressures the intensity of the voltage spikes are still high but a double or multi spikes are obtained. Figure 6 (j) shows the typical voltage and current traces for a discharge at a pressure of 0.3 torr. As can be seen from figure 6 (j), there are two peaks in the voltage waveform. The first peak is characterized by one sharp spike at $6\mu\text{s}$ and has approximately $0.2 - 0.3\mu\text{s}$ duration. The second peak occurs $1.5\mu\text{s}$ later and is characterized by a broad pulse of about $0.1 - 0.2\mu\text{s}$ duration.

Measurement of X-ray emissions from PF device

The diagnostic used to record the X-ray emissions in the dense PF is a PIN diode X-ray covered by different thicknesses of Al foil. The signals recorded by this technique provide information on the time evolution of the X-rays in the PF and they are used to determine the electron temperature of the plasma by the X-ray foil absorption technique [8]. the experimental results of these detection cleared that, good signals are obtained at $V_{ch}= 8\text{ kV}$ and $P= 0.7\text{ Torr}$. Figure 7(a) and (b) show examples of X-ray signals obtained at operating pressures of 0.7 and 0.8 torr respectively. For measurement of soft X-ray intense, the emission from the PF operated with argon is investigated by using a PIN-diode and the pin diode was placed at different places far from the upper end of the anode at 140 mm in the side-on direction.



(a)



(b)

Fig.7 Typical waveforms of the discharge voltage (upper trace) and X-ray signal (lower trace) with Al filter of (a) $12\mu\text{m}$ thickness, (time scale $1\mu\text{S}/\text{div}$) (b) $24\mu\text{m}$ thickness, (time scale $1\mu\text{S}/\text{div}$).

Figures (7 (a and b)) show respectively a sample of typical X-ray signals detected by pin diode with two different Al filters of 12 μm and 24 μm thickness. And discharge voltage for Argon gas at optimum operation conditions. As can be seen from these figures that the pulse of X-ray emission is a short pulse have been registered during and close to the voltage spike and represent the X-ray's signals and the pulse duration (FWMH) is on the order of 0.3 μs or less. This radiation is probably due to bremsstrahlung from the thermal electrons in the plasma.

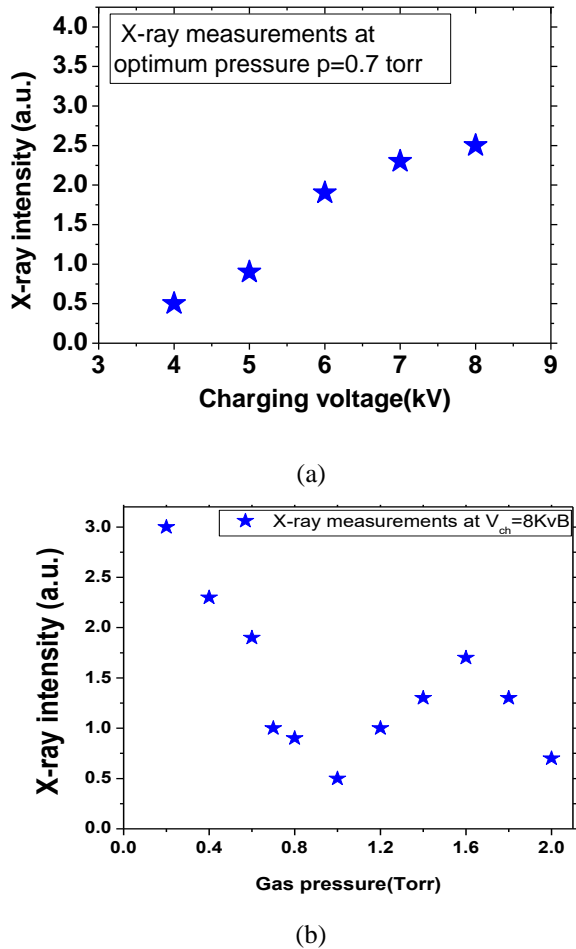


Fig.8 The relative X-ray output from a dense PF is plotted versus (a) the charging voltage of the capacitor bank (b) Argon gas filling pressure within 0.2-2 torr pressure range

The X-ray emission intensity and its characteristics depend on gas type, gas pressure, stored energy electrode materials and shape. The relative X-ray output from a dense PF is plotted versus the voltage of the charging voltage as shown in figure 8. These data were taken with a PIN detector with a 24 μm aluminum filter and optimum argon gas pressure was 0.7 torr. The distribution of the X-ray emission from the focus device varies with the operating voltage. The radiation distribution is a strong function of the acceleration

of charged particles which is, in turn, affected by the electric field during a disruption of focus column. At higher voltages, more X-rays are produced because more charged particles are accelerated to higher energies.

Electron temperature measurements from the PF device

In order to estimate the electron temperature radiated from the PF device, in this experiment the electron temperature have been estimated by using the relative intensity of the light emission from a plasma of argon gas at different pressure and at a charging voltage of 8 kV. Different types of radiation are emitted from hot plasma, and these radiations include electromagnetic radiation, neutron, electron and ion beam as well as high-energy neutral particles (such as atoms and molecules). Plasma emits electromagnetic radiation in a broad frequency range; this radiation includes the line radiation as well as the continuum radiation [9].

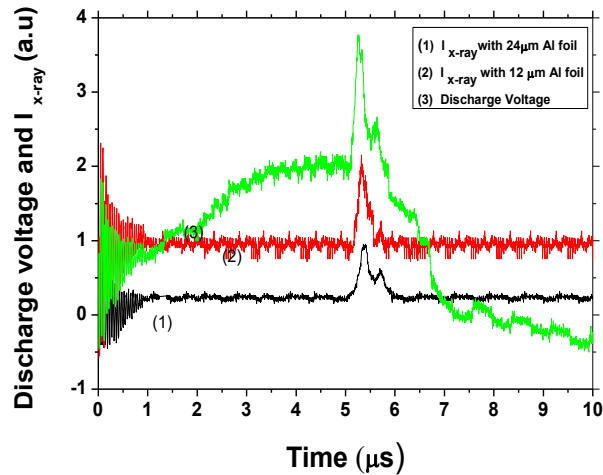


Fig.9. the ratio of the intensity emission transmitted through 12 μm and 24 μm Al foil.

The specific intensity (I_λ) at any particular wavelength λ (and $E=hc/\lambda$) Transmitted through absorbing foils thickness D_j with an absorption coefficient K_j is given by the product of the bremsstrahlung emission and the foil transmission as

$$I_\lambda \propto \lambda^{-2} (kT)^{-1/2} \exp \left[-E/kT - \sum_j K_j(E) D_j \right] \quad (1)$$

Where the subscript j refers to the various foil materials

The values of Eq.(1) have been computed for various foil materials and thicknesses in mg/cm^2 and for electron temperature in eV. In this case the value of Eq.(1) was plotted automatically versus wavelength, and the results are shown in figure 10. Such graph is useful in determining the wavelength region observed, thereby assuring the avoidance of regions of characteristic line radiation and recombination edges. the normalized total transmission, given by the integral of Eq.(1) divided by the integral over the incident bremsstrahlung radiation ($D_j=0$), is plotted versus foil

thickness for various temperature in figure 10.

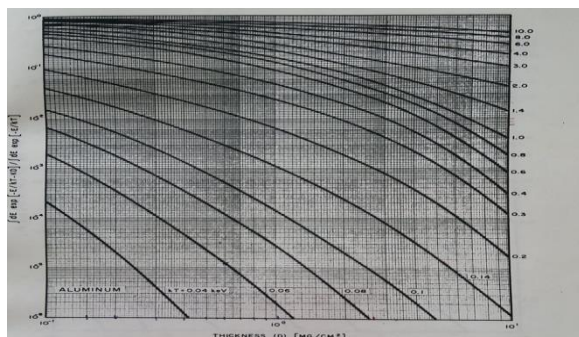


Fig.10. ratio of the integrated bremsstrahlung emission transmitted through foil of the designated material to the total incident flux versus foil thickness (D), for various temperatures. From this the ratio of ordinate value for two different thicknesses may be plotted versus temperature and used for plasma electron temperature determination [10].

It is possible to determine the characteristics of this plasma from the analysis of this electromagnetic radiation emitted from the plasma. The electron temperature using different argon gas pressure (0.3 torr, 0.5 torr, 0.7 torr, 0.9 torr and 1 torr) is found to vary in the range of 0.5 keV to 3keV.

After a series of experiments, we got optimized pressure 0.7 torr at constant voltage 8 kV by using a thickness of Al foil (12 μm Al foil, 24 μm Al foil, 36 μm Al foil and 48 μm Al foil). Our Al foils, which are exactly on the top of the anode tip at distance 14 cm. In case of a distance long of the anode, electron beam from the focus region will interact with surface of anode, so radiation emit from focus and after hitting with the surface of anode is pass through the Al foils thickness.

Preliminary Plasma Focus Applications

The PF effect was carried out on the sample of Polytetrafluoroethylene (PTFE), as a polymer type to improve the surface characterization. Surface morphology of the sample was examined by Scanning electron microscope (SEM), The UV/Vis spectra lead to some measurements for optical band gap energy (E_g) by monitoring of the absorption

edges.

In order to investigate the change in the surface morphology for the pristine and irradiated PTFE by PF, SEM was performed. Figure (11) shows SEM photographs of the pristine and irradiated PTFE with the energy of ion beam was applied. The pristine sample showed a very smooth surface, as shown in Figure (11) [11]. The morphology of the irradiated samples with PF is shown in Figure (11). The SEM photographs of the irradiated samples reveal that there is a change in the morphology as the energies is employed.

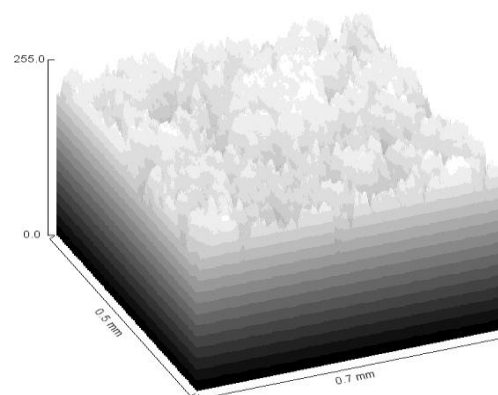
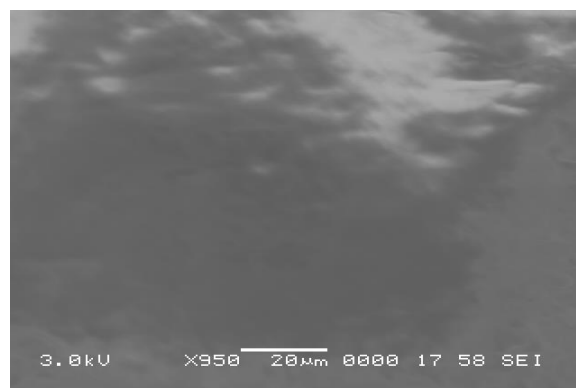


Fig.11 SEM and DIP photographs of a PTFE Sample before exposed to the plasma.

Some cracks are observed in the deposited films at higher shots, which are may be due to thermal shocks developed during ion implantation of 10 shots or may be due to the mismatch between the lattice parameters of the deposited films and substrate. X-Ray Fluorescence (XRF) is a simple analytical technique to investigate which elements are present and their concentrations in the sample under studying. Figure (13) shows the XRF results of the pristine PTFE sample before exposed to 10 shots of the plasma and the major elements concentration is the Rhodium (Rh) and no other elements appear.

Figure (12) and (13) shows the SEM and XRF analysis of the PTFE sample before and after exposed to 10 shots of the plasma focus respectively. As can be seen, figure (13B) show a quite different of the surface of the PTFE sample after exposed to 10 shots of the plasma focus. The results showed that there are new elements deposited on the surface according to XRF analyses after exposed to the plasma for a 10 shots with energy 1K J. The XRF results of the PTFE sample after exposed to the plasma focus shows that the major elements concentrations is the Si which are (51.1056 %), S (21.5161 %), Ca(6.7058 %), Fe (1.7172 %), Cu (10.0475%), Zn(8.9078 %). Other element such as Rh was observed with low concentration which is (0.3851%) as shown in figure (13 B). The main purpose of these coatings is to provide materials with added resistance to wear, corrosion, and oxidation and may also have applications in

electrical and electronic fields [12].

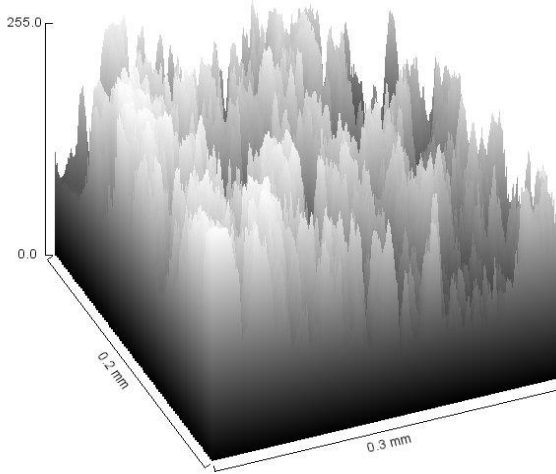
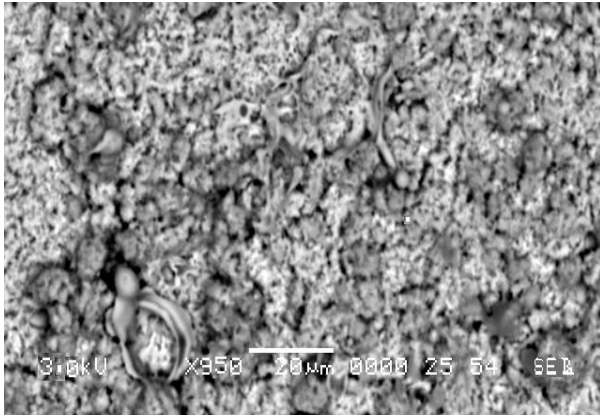
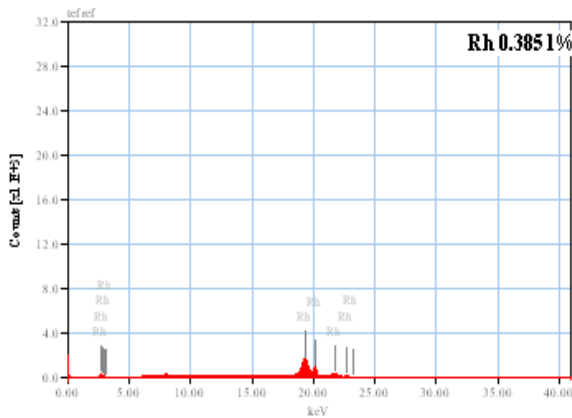
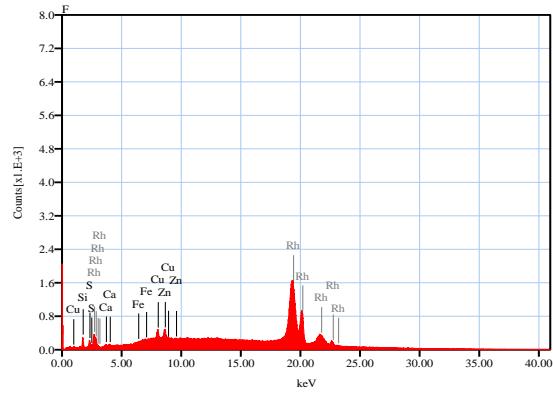


Fig.12 SEM and Digital Imaging Procession Program (DIP) photographs of a PTFE Sample after exposed to the plasma.



(a)



(b)

Fig. 13 (A and B) Typical Energy Dispersive XRF Spectrum of a PTFE sample before and after exposed to the plasma focus respectively.

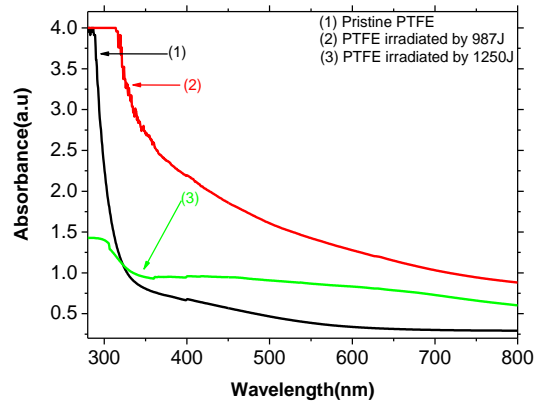


Fig. 14 UV–Vis. spectra of the PTFE (1) pristine sample and (2) and (3) after irradiated by plasma energy of 987J and 1250 J respectively

Ultraviolet and visible (UV/Visible) absorption spectroscopy is the measurement of the attenuation of a beam of light with wavelength after it passes through a sample or after reflection from a sample surface [13]. The results of absorption studies with UV/Vis spectrophotometer were carried out on pristine and irradiated PTFE with plasma at different energies as illustrated in figure (14). Figure (14) shows the (UV/VIS) relation between the wavelength and the absorbance value of the pristine PTFE sample and irradiated to the plasma at different energy. The results showed that the highest shift in absorption wavelength is in the range 290-310 nm (UV/VIS) spectroscopy has become an important tool to estimate the value of optical energy gap (Eg). The results showed that the highest shift in absorption wavelength is in the range 280-315 nm. From figure (14) it is noticed that the pristine sample has a sharp decrease in absorption with increasing wavelength up to 315 nm followed by a plateau region in its UV/Vis spectrum.

The optical band gap of pristine and various irradiated PET

samples were determined from the UV-Vis spectra. The relation between the optical absorption coefficients α and the photon energy $h\nu$ was given by Mott and Davis [14] as

$$\alpha(h\nu) = \frac{B(h\nu - E_g)^n}{h\nu} \quad (2)$$

Where B is a constant dependent on the transition probability, h is Planck's constant, ν is the frequency of the radiation, and E_g is the optical energy gap. The type of transition responsible for the absorption depends on the value of n an index that can take any of the values 1/2, 3/2, 2, or 3 for direct-allowed, direct-forbidden, indirect-allowed, and indirect forbidden transitions, respectively

The optical absorption coefficient (α) was calculated from the absorbance (A) using the following equation [15]:

$$\alpha(\nu) = 2.303 A/d \quad (3)$$

Where d is the thickness of the sample in centimeter and A is defined by $A = \ln(I_0/I_t)$, where I_0 and I_t are the intensities of incident and transmitted light, respectively. In order to determine the direct optical band gap, α^2 was plotted as a function of photon energy $h\nu$. The value of the optical energy gap E_g was calculated from the intersection of the extrapolated line with the photon energy axis (at $\alpha^2=0$).

4 Conclusion

A PF of Mather-type energized and operating with energy of the order of 1KJ has been designed and constructed. Results using a Cu anode of 40 mm diameter shown pinch evidence. All of the measurements were performed using argon as the filling gas. X-ray emission from plasma focus column is investigated with Argon as the filling gas by using pin-diode detector and the signal of X-ray is determined by using the filtration method (ratio method) from argon plasma focus. The pin-diode detection showed that, for focused Argon plasma, two spikes of X-ray are detected at all different values of gas pressures under consideration and at charging voltage of 8 kV. The first spike is located approximately at the maximum compression of plasma focus position, while the second spike is presented immediately after plasma column disruption i.e. after a libration of energetic ion and electron beams. The electron temperature of PF in argon in a focus device of Mather-type energized by a 30.84 μ F, (\approx 1kJ) bank capacitors, was determined for a small amount of X-ray signal measurements. The plasma electron temperature was found to be 0.5–3 keV for hot argon plasma. The surface morphology of the pristine and irradiated PTFE was observed by SEM. The results are discussed in the light of changes in the physical properties of the pristine polymers as a result of their exposure to the plasma produced from the PF device. The irradiated as well as the un-irradiated PTFE films were studied by the XRF technique.

References

- [1] L. K. Lim, S. L. Yap*, and C. S. Wong, Energetic Ion Beam Production by a Low-Pressure Plasma Focus Discharge, AIP Conf. Proc. 1328, 155 (2011)
- [2] Chee Mang Ng, Siew Pheng Moo, and Chiow San Wong, Variation of Soft X-Ray Emission with Gas Pressure in a Plasma Focus, I IEEE Transactions on plasma science, Vol. 26, No. 4, August 1998
- [3] A Bernard et al, Scientific status of plasma focus research, J. Moscow Phys.Soc.8 (1998) 93-170.
- [4] Sing Lee and Adrian Serban, Dimensions and Lifetime of the Plasma Focus Pinch, IEEE Transactions on plasma science, Vol. 24, No. 3, June 1996.
- [5] Leopoldo Soto, New trends and future perspectives on plasma focus research, Plasma Phys. Control. Fusion 47 (2005) A361–A381
- [6] Muhammad Zubair Khan , Yap Seong Ling, and Wong Chiow San, The impact of plasma interference profile (PIP) on argon discharge in plasma focus device , international journal of physical science, Vol. 8(8), pp. 286-294, 28 February, 2013.
- [7] S. Lee, R. S. Rawat, P. Lee, and S. H. Saw, Soft x-ray yield from NX2 plasma focus, Journal of Applied Physics 106, 023309_2009
- [8] G.M. El-kashef, Development of 2.2 kJ Plasma Focus Device and its Operation in various gases, Sch. J. Eng. Tech., 2014; 2(3A):360-366
- [9] Sh. Al-Hawat • M. Akel • C. S. Wong, X-ray Emission from Argon Plasma Focus Contaminated with Copper Impurities in AECS PF-2 Using Five Channel Diode Spectrometer, J Fusion Energ (2011) 30:503–508.
- [10] Elton, R.C. Determination of Electron Temperature Between 50 eV and 100 keV From X-Ray Continuum Radiation in Plasma ,NRL Report 6738, Washington, D.C.11 1968.
- [11] M.Elgarhy, plasma focus and its applications, M.Sc thesis, Al-Azhar university, faculty of science, department of physics, cairo 2010.
- [12] F.diab, "Experimental Studies of Electrothermal Plasma Gun" Ph.D Thesis, Physics Dept. - Faculty of Science, Al-Azhar University - Cairo (2013).
- [13] Andreas Schutze , Jeong, J.Y Babayan, S.E. Jae young Park, Selwyn, G.S. Hicks; IEEE Trans. Plasma Science; 26, 1685 (1998).
- [14] G. Shiv Prasad, De.Abhijit and De udayan; International Journal of Spectroscopy, PP 1- 7 (2011).
- [15] A. Chapiro, Radiation Chemistry of Polymeric System, Interscience Publishers, London, p.354, (1962).